Cellular/Molecular

Dual Effects of 5-HT$_{1a}$ Receptor Activation on Breathing in Neonatal Mice

Andrea E. Corcoran,[1,2,3] **Kathryn G. Commons,**[4] **Yuanming Wu,**[7] **Jeffrey C. Smith,**[5] **Michael B. Harris,**[1] **and George B. Richerson**[2,6,7]

[1]Department of Biology and Wildlife, University of Alaska Fairbanks, Fairbanks, Alaska 99775, [2]Departments of Neurology and Cellular and Molecular Physiology, Yale University, New Haven, Connecticut 06520, [3]Department of Physiology and Neurobiology, Geisel School of Medicine at Dartmouth, Lebanon, New Hampshire 03756, [4]Department of Anesthesia, Perioperative and Pain Medicine, Boston Children's Hospital, Boston, Massachusetts 02115, [5]Cellular and Systems Neurobiology Section, National Institute of Neurological Disorders and Stroke, National Institutes of Health, Bethesda, Maryland 20892, [6]Veteran's Affairs Medical Center, Iowa City, Iowa 52242, and [7]Departments of Neurology, and Molecular Physiology and Biophysics, University of Iowa, Iowa City, Iowa 52242

Inhibitory 5-HT$_{1a}$ receptors are located on serotonin (5-HT) neurons (autoreceptors) as well as neurons of the respiratory network (heteroreceptors). Thus, effects on breathing of 5-HT$_{1a}$ agonists, such as (*R*)-(+)-8-hydroxy-2-(di-*N*-propylamino) tetralin (8-OH-DPAT), could either be due to decreased firing of 5-HT neurons or direct effects on the respiratory network. Mice in which the transcription factor LMX1B is genetically deleted selectively in *Pet1*-1-expressing cells (*Lmx1b$^{f/f/p}$*) essentially have complete absence of central 5-HT neurons, providing a unique opportunity to separate the effect of activation of downstream 5-HT$_{1a}$ heteroreceptors from that of autoreceptors. We used rhythmically active medullary slices from wild-type (WT) and *Lmx1b$^{f/f/p}$* neonatal mice to differentiate autoreceptor versus heteroreceptor effects of 8-OH-DPAT on hypoglossal nerve respiratory output. 8-OH-DPAT transiently increased respiratory burst frequency in *Lmx1b$^{f/f/p}$* preparations, but not in WT slices. This excitation was abolished when synaptic inhibition was blocked by GABAergic/glycinergic receptor antagonists. Conversely, after 10 min of application, frequency in *Lmx1b$^{f/f/p}$* slices was not different from baseline, whereas it was significantly depressed in WT slices. In WT mice *in vivo*, subcutaneous injection of 8-OH-DPAT produced similar biphasic respiratory effects as in *Lmx1b$^{f/f/p}$* mice. We conclude that 5-HT$_{1a}$ receptor agonists have two competing effects: rapid stimulation of breathing due to excitation of the respiratory network, and delayed inhibition of breathing due to autoreceptor inhibition of 5-HT neurons. The former effect is presumably due to inhibition of inhibitory interneurons embedded in the respiratory network.

Key words: **8-OH-DPAT; Lmx1b; serotonin**

Introduction

5-HT$_{1a}$ receptors are located throughout the respiratory network, on both 5-HT source neurons of the raphe and on downstream neurons of target nuclei. These receptors are coupled to inhibitory G-proteins. Thus ligand binding to somatodendritic 5-HT$_{1a}$ autoreceptors inhibits firing of 5-HT neurons, reducing 5-HT release and therefore decreasing activation of other receptors by endogenous 5-HT (McCall and Clement, 1989; Sharp et al., 1989; Veasey et al., 1995). 5-HT$_{1a}$ heteroreceptors are found in several respiratory-related nuclei including the hypoglossal motor nucleus, the retrotrapezoid nucleus, and the pre-Bötzinger complex (preBötC; Okabe et al., 1997; Liu and Wong-Riley, 2010), and there has been much interest in pharmacological targeting of these receptors to reverse life-threatening instabilities of breathing in clinical conditions (Wilken et al., 1997; El-Khatib et al., 2003; Richter et al., 2003; Manzke et al., 2009). Determining the effect of these downstream 5-HT$_{1a}$ receptors on the output of the respiratory network, however, is challenging when studied in an intact network because it is not always clear whether the target neurons cause excitation or inhibition of respiratory output. Additionally, the agonists and antagonists used to query the role of 5-HT$_{1a}$ receptor function can have nonspecific, off-target effects.

Much of our knowledge describing the role of 5-HT$_{1a}$ receptors in control of breathing has been based on studies using 8-OH-DPAT, which binds to both 5-HT$_{1a}$ autoreceptors and downstream heteroreceptors, making it difficult to differentiate between the role of the two receptor populations. Additionally, 8-OH-DPAT has moderate affinity for 5-HT$_7$ receptors (Bard et al., 1993; Eriksson et al., 2008). Low levels of mRNA expression for 5-HT$_7$ receptors are found in the preBötC (Richter et al., 2003) and immunoreactivity has been reported in raphe serotonergic cells (Muneoka and Takigawa, 2003). Our knowledge of the role of 5-HT$_7$ receptors in breathing is limited, although they

Received Feb. 26, 2013; revised Oct. 29, 2013; accepted Nov. 2, 2013.

Author contributions: A.E.C., K.G.C., J.C.S., M.B.H., and G.R. designed research; A.E.C., K.G.C., and Y.W. performed research; A.E.C. and K.G.C. analyzed data; A.E.C., J.C.S., M.B.H., and G.B.R. wrote the paper.

This work was supported in part by the Intramural Research Program of the NIH, NINDS, and from the NIH Grants 2U54NS041069, NIH/NICHD, P01HD36379, and R01HD052772.

The authors declare no competing financial interests.

Correspondence should be addressed to Dr. Andrea E. Corcoran, Department of Physiology and Neurobiology, Geisel School of Medicine at Dartmouth, 1 Medical Center Drive, Lebanon, NH 03756. E-mail: andrea.e.corcoran@dartmouth.edu.

DOI:10.1523/JNEUROSCI.0864-13.2014

 0270-6474/14/340051-09$15.00/0

appear to be involved in restoring phrenic nerve activity following fentanyl-induced depression of respiratory discharge (Richter et al., 2003). The potential facilitation of respiration by activation of 5-HT$_7$ receptors could confound interpretation of the effects of 8-OH-DPAT on both 5-HT$_{1a}$ autoreceptors and heteroreceptors.

Here we report a unique approach to distinguish between 5-HT$_{1a}$ receptor populations in which we use mice lacking central 5-HT neurons (*Lmx1b*$^{f/f/p}$ mice). Recent investigation into the importance of the 5-HT system in ventilatory chemosensation has exploited the use of this transgenic mouse (Ding et al., 2003; Zhao et al., 2006; Hodges and Richerson, 2008b; Hodges et al., 2008; Buchanan and Richerson, 2010). An experimental benefit of the loss of central 5-HT neurons in this mouse model is the coincident loss of 5-HT$_{1a}$ autoreceptors, but not heteroreceptors. As such, application of 8-OH-DPAT in *Lmx1b*$^{f/f/p}$ mice will only affect heteroreceptor populations, providing a tool to identify the role of these receptors by comparing the results with those obtained from WT mice in which 5-HT$_{1a}$ autoreceptors and downstream heteroreceptors are both present. Additionally, we examined the effect of coadministered 8-OH-DPAT with a 5-HT$_7$ receptor antagonist, removing potential confounding effects of 5-HT$_7$ receptors in interpretation of the role of 5-HT$_{1a}$ receptors in breathing.

Materials and Methods

5-HT neuron-deficient mouse model. LMX1b is a transcription factor that is required for 5-HT neuron differentiation during embryogenesis (Ding et al., 2003). The procedure using Cre-Lox site-specific recombination targeting this transcription factor to produce mice lacking 5-HT neurons (*Lmx1b*$^{f/f/p}$ mice) has been previously described by Zhao et al. (2006). Briefly, females homozygous for the Lmx1b sequence flanked by LoxP (floxed *Lmx1b*;*Lmx1b*$^{f/f}$) are mated with males homozygous for floxed *Lmx1b* and hemizygous for *ePet1-Cre* (*Lmx1b*$^{flox/flox,ePet-Cre/+}$, also referred to as *Lmx1b*$^{f/f/p}$). This strategy results in a 1:1 ratio of *Lmx1b*$^{f/f}$ (referred to here as WT; containing a normal number of central 5-HT neurons that are phenotypically normal) and *Lmx1b*$^{f/f/p}$ pups (expressing loxP sites flanking both *Lmx1b* alleles, targeted by Cre recombinase produced specifically in *Pet1*-expressing cells, and missing >99% of central 5-HT neurons). Genotyping was performed on tail tissue samples obtained from each mouse and using procedures described by Zhao et al. (2006). All experiments were performed on neonatal mice, or on slice preparations derived from neonatal mice [postnatal day (P)0–P4], to allow for direct comparison between the various methods used. Note that use of the *in vitro* medullary slice preparation is typically used at this age due to instability of the respiratory-related activity and lower viability of slice preparations from older animals.

Tryptophan hydroxylase immunohistochemistry. Brainstems were fixed overnight in 4% paraformaldehyde in 0.1 M phosphate buffer (containing the following in g/L: NaH_2PO_4 3.18, Na_2HPO_4 10.94, pH 7.4), allowed to sink in cryoprotectant [30% sucrose in PBS containing the following in g/L: NaCl 87, NaH_2PO_4 (monobasic) 3.86, Na_2HPO_4 (dibasic) 10.2] for 24 h, frozen, and cut into 30-μm-thick sections (WT $n = 6$, 3.2 ± 0.3-d-old; *Lmx1b*$^{f/f/p}$ $n = 7$, 3.0 ± 0.3-d-old). Consecutive coronal sections were mounted on microscope slides and stained for tryptophan hydroxylase (TpOH) as follows: sections were rinsed in PBS, incubated for 30 min in 0.15% H_2O_2 in methanol, for 5 min in PBS with 0.1% Triton X-100 (PBST), for 60 min in PBST with 5% horse serum, and overnight at room temperature in PBST with 2.5% horse serum and a primary antibody against TpOH (Sigma-Aldrich, T0678; 1:1000 dilution). Sections were rinsed three times in PBST, incubated for 30 min in biotinylated anti-mouse IgG antibody (1:250 dilution) in PBST with 2.5% horse serum, and rinsed three times in PBST. Sections were then processed using the avidin-biotin-peroxidase method with the Vectastain ABC kit (Vector Laboratories), and washed three times in PBS. Serotonin neurons were visualized using NovaRED (Vector Laboratories) as the chromogen, and washed three times in water. Sections were dehydrated with an ethanol series, cleared with xylenes, and coverslipped using Permount (Fisher Scientific). Stained sections were observed with brightfield illumination.

The number of TpOH-positive neurons was counted in every available and intact section between −1.8 to 2.8 mm rostral to obex. Within each section, TpOH-positive neuron counts were made from two regions: a midline region containing nucleus raphe obscurus and pallidus (identified by a 0.5-mm-wide rectangle centered on the midline; Hodges et al., 2011) and a bilateral ventrolateral medulla region that included any neurons not located within the midline rectangle. For each animal, the total number of cells counted from all sections was divided by the number of sections examined, resulting in an average number of cells/section for each individual animal. These were then averaged for WT and *Lmx1b*$^{f/f/p}$. Differences between the average number of positive cells per section in WT and *Lmx1b*$^{f/f/p}$ were determined using a Mann–Whitney rank sum test with $p < 0.05$ as significant.

5-HT$_{1A}$ receptor autoradiography. P3 mice were decapitated and the brains were rapidly removed and frozen. Brains were sectioned 20 μm thick using a cryostat and slices were thaw mounted on Superfrost Plus slides (Fisher Scientific). Slides were maintained at −80°C until processing. For 5-HT$_{1a}$ receptor autoradiography, slides were preincubated for 30 min at room temperature in 0.17 M Tris-HCl buffer, pH 7.6, containing 4 mM $CaCl_2$ and 0.01% ascorbic acid. For total binding, slides were incubated for 1 h at room temperature in the same buffer with the addition of 4 nM ^{3}H-8-OH-DPAT (New England Nuclear) and 10 μM pargyline. Nonspecific binding was determined by processing slides similarly except 10 μM 5-HT was added as a displacer for ^{3}H-8-OH-DPAT. Sections were subsequently rinsed, dried and exposed to BAS-TR2025 phosphoimaging plates (Fujifilm Medical Systems) for 3 weeks with a set of ^{3}H-standards (GE Healthcare). Quantitative densitometry was completed using NIH ImageJ software.

Eight WT (5 females and 3 males) and 8 *Lmx1b*$^{f/f/p}$ (2 females and 6 males) were analyzed. Every fourth section was processed for specific binding and serial sections were processed for nonspecific binding. For each area analyzed, specific binding was measured on three sections per mouse; nonspecific binding was measured on the three serial sections. Three areas in the medulla were analyzed: caudal raphe (CR) consisting of an area 0.5 mm wide centered on the midline, and lateral to that the caudal ventrolateral medulla (CVL). The spinal nucleus of V (Sp5) was also sampled. Mean specific binding was determined per mouse and these were averaged together to generate a group mean. Nonspecific binding values were subtracted from those of total binding to obtain specific binding. For each area, differences between WT and *Lmx1b*$^{f/f/p}$ were determined using a Student's *t* test with $p < 0.05$ as significant.

In vivo *plethysmography.* Whole-body plethysmography was used to measure ventilation in P2 mice (described previously by Hodges et al., 2009). In neonates, this method allows for unrestrained breathing measurements, resulting in less stress and accurate determination of breathing frequency and relative tidal volume; however, it does not allow for accurate calculation of absolute tidal volume (which is thus expressed as relative to baseline; for review, see Cummings et al., 2004). Pups were separated from their mother and placed in a 9 ml Plexiglas chamber equipped with inflow and outflow gas ports, a pressure transducer, and a temperature sensor. Ambient temperature was maintained at 30°C using a temperature controller (TCAT-2AC, Physitemp Instruments) and an incandescent, infrared lamp. Pressure transducer data were digitized at 100 Hz using an analog-to-digital converter (PCI-6224, National Instruments) and recorded using MATLAB data acquisition software (MathWorks) with a custom-written programs used to monitor data in real-time and analyze off-line.

Studies consisted of a stop flow protocol, where room air flowed through the chamber for 20 s and was stopped for 60 s (repeated five times). This method allows for low noise recording of small amplitude breaths generated by neonatal mice. Baseline ventilatory measurements were made before (baseline), and 30, 60, and 120 min following subcutaneous (intrascapular) injection of 8-OH-DPAT (Sigma-Aldrich; 100 μg/kg body weight, dissolved in 150 mM NaCl). Pups were in the chamber for ~7 min at a time, and returned to their mother between record-

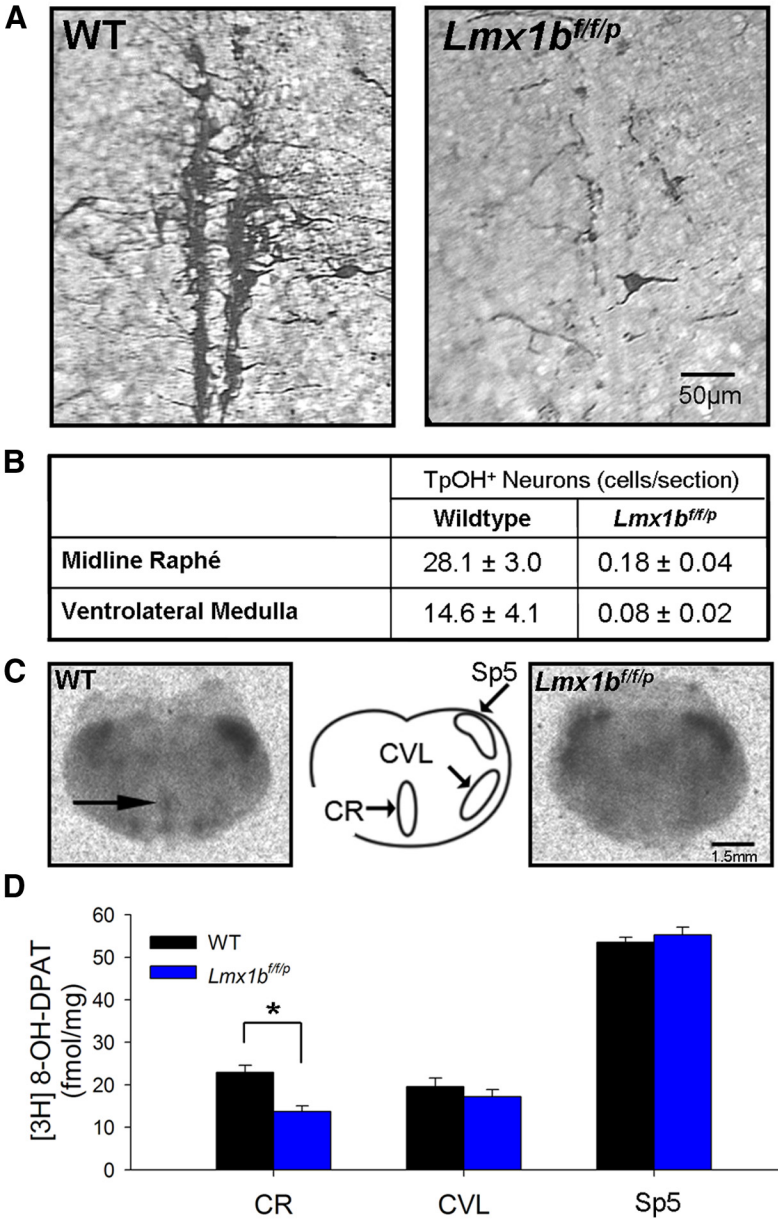

	TpOH+ Neurons (cells/section)	
	Wildtype	*Lmx1b*$^{f/f/p}$
Midline Raphé	28.1 ± 3.0	0.18 ± 0.04
Ventrolateral Medulla	14.6 ± 4.1	0.08 ± 0.02

Figure 1. 5-HT neurons and 5-HT$_{1a}$ receptor binding are specifically lost within the caudal raphe of *Lmx1b*$^{f/f/p}$ mice. ***A***, Transverse sections of the caudal medulla from P2 WT and *Lmx1b*$^{f/f/p}$ mice immunostained for TpOH-positive neurons. ***B***, Neuron counts (average no. TpOH-positive neurons/section; $n = 6$ WT, $n = 7$ *Lmx1b*$^{f/f/p}$) revealed a significant depletion of 5-HT neurons in *Lmx1b*$^{f/f/p}$ mice in both the midline raphe and ventrolateral medulla regions. Note that sections were 30 μm thick. ***C***, Autoradiographs of transverse sections through the medulla from P3 WT and *Lmx1b*$^{f/f/p}$ mice illustrating distribution of 5-HT$_{1a}$ receptor binding. In WT mice, binding was seen in the midline (arrow) in the area of the CR that was not apparent in *Lmx1b*$^{f/f/p}$ mice. ***D***, Quantification revealed *Lmx1b*$^{f/f/p}$ mice had significantly less 5-HT$_{1a}$ receptor binding than WT mice in the CR, but there was no difference in receptor binding in the CVL or Sp5 ($n = 8$ WT, $n = 8$ *Lmx1b*$^{f/f/p}$). *Significant difference between genotypes; $p < 0.05$, *t* test. Data are mean ± SEM.

ings. Data are presented as mean ± SEM. Differences were determined using a two-way repeated-measures (RM) ANOVA with Bonferroni *post hoc* analysis for multiple comparisons with statistical significance attributed to $p < 0.05$.

In vitro *medullary slice preparations.* Experiments were performed on brainstem slices prepared from neonatal mice (P0–P4). Mice were decapitated, and the brainstem and spinal cord removed under a flow of chilled dissection solution composed of the following (in mM): 124 NaCl, 25 $NaHCO_3$, 3 KCl, 1.5 $CaCl_2$, 1.0 $MgSO_4$, 0.5 NaH_2PO_4, 30 D-glucose, and equilibrated with 95% O_2 and 5% CO_2, pH ~7.4. The brainstem was pinned to a wax block, and transverse slices of the medulla (500–600 μm thick) were prepared using a vibratome (Smith et al., 1991). Slices from the rostral medulla containing the preBötC, the hypoglossal motor nucleus, the most rostral hypoglossal nerve rootlets and 5-HT neurons of the medullary raphe (Ptak et al., 2009) were placed in a recording chamber with a volume of 0.7 ml and superfused with dissection solution at a rate of 0.7 ml/min via a syringe pump (Harvard Apparatus). The temperature of aCSF within the chamber was increased to 29°C using a temperature controller (Warner Instruments; TC-324B). After stabilization of the slice, the potassium concentration in recording solutions was elevated to 8 mM to enhance rhythmic activity in the slice, as per standard procedures (Smith et al., 1991; Ptak et al., 2009).

Inspiratory-related motor discharge of the hypoglossal rootlets was recorded continuously using glass suction electrodes. Signals were amplified × 10,000 and bandpass filtered (0.3–1 kHz) using a Grass LP511 AC amplifier (Grass Technologies). A Hum Bug noise eliminator (Quest Scientific) was used as a digital filter of 60 Hz noise. Data were digitized at 10 kHz, stored on a computer hard drive and analyzed off-line using MATLAB software. Analysis of hypoglossal root discharge included full wave rectification, integration, and calculation of the moving average with a bin size of 50 ms.

After 30 min of baseline recording, the superfusate was switched to one containing one of the drugs listed below and applied continuously to the slice for 10 min, which was sufficient to achieve steady-state responses in the recorded hypoglossal nerve activity. The last 2 min under each condition (control and drug application) was used to measure values of each parameter to determine the effect of drug relative to baseline ("steady-state" response). We also analyzed a "peak" response in all slices exposed to 8-OH-DPAT, defined as the maximum hypoglossal burst frequency observed for any 1 min time period during the 10 min exposure. Only one slice was taken and recorded from each animal and a 2 min average value for each condition and/or parameter was used from each slice for quantitative analyses. Data are presented as mean ± SEM. Differences were determined using a two-way RM ANOVA with Bonferroni *post hoc* analysis for multiple comparisons or a Student's paired *t* tests and statistical significance was attributed to $p < 0.05$. Each slice was exposed to a single drug, with the exception of the coapplication of 8-OH-DPAT and SB 269970, and coapplication of 8-OH-DPAT and a gabazine/CGP 55845/strychnine mixture to block endogenous $GABA_A$, $GABA_B$, and glycine receptors, respectively.

Results

5-HT neuron and 5-HT$_{1a}$ receptor distributions in Lmx1b$^{f/f/p}$ mice

As reported by Zhao et al. (2006) and Ding et al. (2003), we found near-complete absence of 5-HT neurons in neonatal *Lmx1b*$^{f/f/p}$ brainstems. Immunohistochemical staining identified a very small number of TpOH-positive neurons. An average of 0.18 ± 0.04 TpOH-positive neurons per section was counted in the midline raphe region of P2 *Lmx1b*$^{f/f/p}$ pup medullary tissue, compared with 28.1 ± 3 in WT (Fig. 1*A*,*B*), representing a >99%

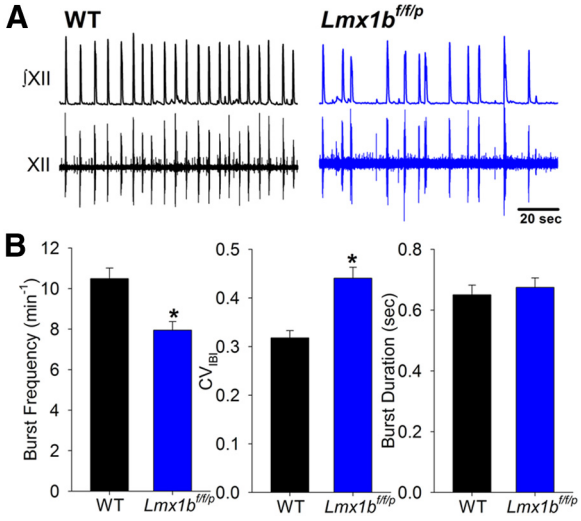

Figure 2. Hypoglossal nerve bursting was slow and irregular in *Lmx1b*$^{f/f/p}$ mouse pup rhythmogenic slice preparations. ***A***, Traces of raw hypoglossal (XII) and integrated XII (∫XII) nerve activity in WT and *Lmx1b*$^{f/f/p}$ slices under control conditions. ***B***, XII burst frequency was lower in *Lmx1b*$^{f/f/p}$ preparations. Bursting was also more irregular in *Lmx1b*$^{f/f/p}$ preparations than WT, as quantified by the coefficient of variation of the interburst interval (CV_{IBI}). Burst duration was the same in both genotypes ($n = 51$ WT, $n = 46$ *Lmx1b*$^{f/f/p}$).*Significant difference between genotypes; $p < 0.05$, *t* test. Data are mean ± SEM.

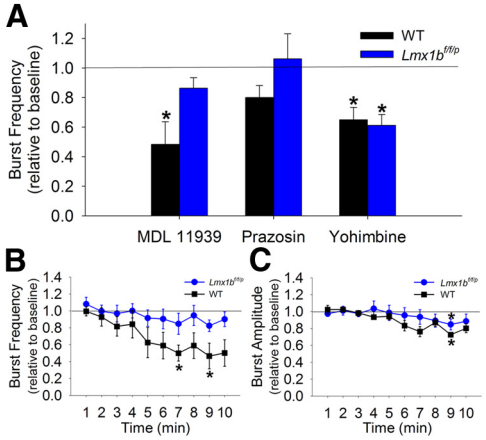

Figure 3. There was no evidence for endogenous 5-HT release in *Lmx1b*$^{f/f/p}$ slices, or compensation by an increase in adrenergic tone. ***A***, MDL 11939 (selective 5-HT$_{2a}$ receptor antagonist; 50 μM) significantly decreased hypoglossal burst frequency in WT rhythmogenic slices ($p = 0.004$, $n = 6$ WT) but not in *Lmx1b*$^{f/f/p}$ slices ($p = 0.234$, $n = 7$ *Lmx1b*$^{f/f/p}$; two-way RM ANOVA followed by Bonferroni test for multiple comparisons). No differences were observed between genotypes in the responses to prazosin hydrochloride (α1 receptor antagonist; 50 μM; $n = 6$ WT, $n = 6$ *Lmx1b*$^{f/f/p}$) or yohimbine hydrochloride (α2 receptor antagonist; 50 μM; $n = 6$ WT, $n = 6$ *Lmx1b*$^{f/f/p}$; two-way RM ANOVA followed by Tukey test for multiple comparisons; $p < 0.001$). ***B***, ***C***, Time course of burst frequency (***B***) and burst amplitude (***C***; relative to baseline) during a 10 min bath application of MDL11939 (50 μM) in WT and Lmx1b$^{f/f/p}$ preparations (Friedman RM ANOVA on ranks followed by Dunn's methods for multiple comparisons; $p < 0.001$). *Significant difference from baseline. Data are mean ± SEM.

depletion in *Lmx1b*$^{f/f/p}$ mice ($p < 0.001$). A similar reduction was observed in the ventrolateral medullary region ($p < 0.001$). We also evaluated 5-HT$_{1a}$ receptor binding sites in neonatal *Lmx1b*$^{f/f/p}$ tissue using quantitative tissue autoradiography. In nonraphe areas, such as the Sp5 and the CVL, WT and *Lmx1b*$^{f/f/p}$ mice had equivalent levels of 5-HT$_{1a}$ receptor binding. However, there was selective loss of 5-HT$_{1a}$ receptor binding along the midline in the area occupied by the caudal raphe nuclei in *Lmx1b*$^{f/f/p}$ compared with WT mice (Fig. 1*C*,*D*). Note that the nonraphe areas (CVL and Sp5) are where downstream heteroreceptors are located and the raphe area (CR) is where we expect somatodendritic autoreceptors and possibly downstream 5-HT$_{1a}$ receptors.

Respiratory discharge in the rhythmogenic medullary slice

Hypoglossal motor output was characterized in *Lmx1b*$^{f/f/p}$ slices. Because 5-HT is an excitatory modulator for breathing, the loss of excitatory drive might cause *Lmx1b*$^{f/f/p}$ slice preparations to be incapable of bursting (particularly because these slice preparations are devoid of many normal inputs and modulators). Hypoglossal nerve bursting was present, although it was slower in *Lmx1b*$^{f/f/p}$ (7.9 ± 0.42 bursts/min; $n = 46$) compared with WT preparations (10.499 ± 0.52 bursts/min; $n = 51$; Fig. 2; $p < 0.001$). Additionally, the burst pattern in *Lmx1b*$^{f/f/p}$ slices was more irregular than WT slices as assessed by an elevated (~42%) coefficient of variation of the interburst interval (CV_{IBI}; Mann–Whitney rank sum test; $p < 0.001$). Burst duration was equivalent between genotypes (0.65 ± 0.03 and 0.67 ± 0.03 s).

In brain slices from WT mice, hypoglossal nerve output is dependent on continuous activation of 5-HT$_{2A}$ receptors by endogenous 5-HT (Peña and Ramirez, 2002; Ptak et al., 2009). To ensure that endogenous 5-HT was indeed absent in *Lmx1b*$^{f/f/p}$ slices, we bath-applied MDL 11939 (MDL; α-Phenyl-1-(2-phenylethyl)-4-piperidine methanol; Tocris Bioscience), a highly selective 5-HT$_{2a}$ receptor antagonist, to the preparation (50 μM, dissolved in 0.1% DMSO in aCSF; $n = 7$). There were no significant effects on burst frequency (Fig. 3; $p = 0.234$), although a mild reduction in burst amplitude was observed. This is in contrast to effects of MDL in WT slices ($n = 6$), which resulted in a marked depression of burst activity (~50%; $p = 0.004$), as previously reported by Ptak et al. (2009). We thus conclude that these slices lack endogenous 5-HT and activation of 5-HT$_{2a}$ receptors.

Because the *Lmx1b*$^{f/f/p}$ slice, devoid of 5-HT, retains some (albeit altered) rhythmogenic activity, whereas respiratory output is blocked by 5-HT$_2$ receptor antagonists in WT mice (Peña and Ramirez, 2002; Ptak et al., 2009; Viemari et al., 2011), we hypothesized that there may be a compensatory mechanism or altered network that provides an alternative source of excitation. We thus examined whether there were differences in noradrenergic modulation (Viemari et al., 2011) by testing responses to adrenergic antagonists in WT and *Lmx1b*$^{f/f/p}$ mice (Fig. 3*A*). None was detected. Neither genotype showed any significant changes in hypoglossal burst frequency in response to the α1-adrenergic receptor antagonist prazosin hydrochloride (Tocris Bioscience; 50 μM, dissolved in 0.5% DMSO in aCSF; $n = 6$ WT, $n = 6$ *Lmx1b*$^{f/f/p}$). Yohimbine is an antagonist at α2-adrenergic receptors with effects at a variety of 5-HT and other receptors including partial agonist effects at 5-HT$_{1a}$ receptors. Yohimbine hydrochloride (Tocris Bioscience; 50 μM, dissolved in aCSF) depressed frequency in both WT and *Lmx1b*$^{f/f/p}$ mice by a similar degree (to 0.65 ± 0.08 and 0.61 ± 0.07 relative to baseline, respectively; $n = 6$ WT, $n = 6$ *Lmx1b*$^{f/f/p}$). The compensatory mechanism to maintain excitation remains unknown.

Effects of 8-OH-DPAT *in vitro* and *in vivo*

We examined the effect of 8-OH-DPAT *in vitro* and *in vivo* in both WT (containing both 5-HT$_{1a}$ autoreceptors and downstream heteroreceptors) and *Lmx1b*$^{f/f/p}$ neonates (containing only downstream 5-HT$_{1a}$ heteroreceptors). Because *Lmx1b*$^{f/f/p}$ mice lack raphe 5-HT neurons and 5-HT$_{1a}$ autoreceptors, the effect of 8-OH-DPAT in this mouse is due to activation of downstream 5-HT$_{1a}$ receptors alone.

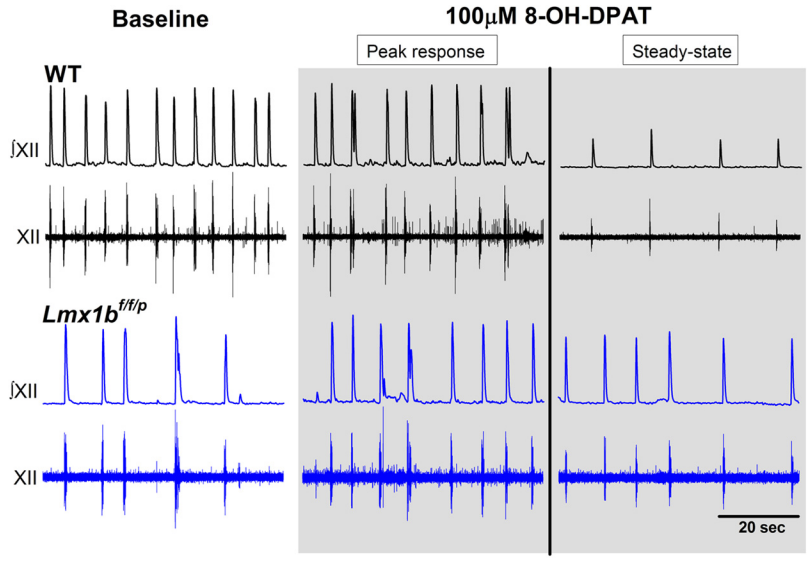

Figure 4. Traces of raw hypoglossal (XII) nerve activity in WT and *Lmx1b*$^{f/f/p}$ slices, before (baseline) and during (peak and steady-state) bath application of 8-OH-DPAT (100 μM). Represented are examples of a transient peak response (defined as the maximum burst frequency during the 10 min drug exposure) and a steady-state response (attained at the end of the 10 min drug application).

We examined the effect of a range of doses of 8-OH-DPAT (Sigma-Aldrich; 10 nM–100 μM, dissolved in aCSF) on hypoglossal nerve bursting activity in slices (Fig. 4). We determined the peak response (the maximum burst frequency observed during the 10 min exposure) and the steady-state response (average of the final 2 min of the 10 min exposure). In slices from WT mice (n = 3, 4, 4, 6, 6, 6, 5 slices for each successive dose of 8-OH-DPAT) burst frequency began to decrease within the first few minutes (Fig. 5*A*), stabilizing below baseline at the end of a 10 min exposure to higher doses (3–100 μM; Fig. 5*B*). Lower doses did not depress burst frequency. Unlike WT slices, *Lmx1b*$^{f/f/p}$ slices (n = 4, 5, 4, 5, 4, 9, 5 for each successive dose in *Lmx1b*$^{f/f/p}$), did not exhibit an attenuation of frequency at any dose. In fact, they responded to 8-OH-DPAT in an opposite manner: with a transient increase in burst frequency (peak response; Fig. 5*C*). This peak response was significant at higher doses (1–100 μM) and was not observed in WT preparations, with the exception of one dose (0.3 μM). 8-OH-DPAT had very little effect on burst amplitude at any dose in either genotype (Fig. 5*D*). Only at 100 μM was burst amplitude significantly lower than baseline in WT preparations (0.57 ± 0.09 relative to baseline; p = 0.022).

In vivo results were similar to those obtained *in vitro* (Fig. 6). Baseline ventilation, as assessed by whole-body plethysmography, was lower in *Lmx1b*$^{f/f/p}$ P2 pups compared with WT pups (n = 7 *Lmx1b*$^{f/f/p}$; n = 7 WT). Breathing was slower in *Lmx1b*$^{f/f/p}$ pups (Fig. 7*A*; average breathing frequency of 2.12 ± 0.17 Hz in *Lmx1b*$^{f/f/p}$ compared with 3.49 ± 0.15 Hz in WT pups). Breaths were approximately half the size of those in WT mice (Fig. 7*B*; 56.7 ± 5.7% of WT; normalized to weight). Additionally, the loss of central 5-HT resulted in unstable breathing (Fig. 7*D*,*E*), with long respiratory pauses (>1 s) and a large percentage of time spent apneic (~17% of the time). These observations are similar to those reported by Hodges et al. (2009) in neonatal *Lmx1b*$^{f/f/p}$ mice.

Subcutaneous injection of 8-OH-DPAT altered breathing differently in the two genotypes (Figs. 6, 7). Although 8-OH-DPAT significantly augmented frequency in *Lmx1b*$^{f/f/p}$ pups 30 min postinjection ($p < 0.001$), there was no change in breathing frequency in WT pups until 2 h postinjection (Fig. 7*A*; p = 0.011). There was a twofold increase in minute ventilation (frequency × amplitude; Fig. 7*B*) in *Lmx1b*$^{f/f/p}$ mice ($p < 0.001$) and a nonsignificant ~20% trend toward a reduction in WT mice (Fig. 7*C*). Stimulation of 5-HT$_{1a}$ receptors also normalized breathing in *Lmx1b*$^{f/f/p}$ pups by reducing the number of apneas (Fig. 7*D*; $p < 0.001$) and percentage time spent apneic (Fig. 7*E*; $p < 0.001$).

Coapplication of 8-OH-DPAT and a 5-HT$_7$ antagonist

One caveat of using 8-OH-DPAT to examine effects of 5-HT$_{1a}$ receptors is that it is a partial agonist at 5-HT$_7$ receptors, thus confounding interpretation. To isolate the effect of 5-HT$_{1a}$ receptors, we coapplied 8-OH-DPAT (3 μM) with the 5-HT$_7$ antagonist SB 269970 hydrochloride (Tocris Bioscience; 20 μM, dissolved in aCSF) to rhythmogenic medullary slices (n = 6 WT; n = 9 *Lmx1b*$^{f/f/p}$). SB 269970 alone did not alter hypoglossal bursting in either type of preparation (Fig. 8). After addition of 8-OH-DPAT to the aCSF containing SB 269970, we examined both peak and steady-state responses. As with 8-OH-DPAT alone, coapplication of 8-OH-DPAT and SB 269970 did not evoke an increase in hypoglossal burst frequency in WT slices. In contrast, coapplication resulted in a transient increase in *Lmx1b*$^{f/f/p}$ preparations (from 3.78 ± 0.59 bursts/min to 5.00 ± 0.53 bursts/min; p = 0.003). For both genotypes, the steady-state responses to the coapplication were similar to effects of 8-OH-DPAT alone; a decrease in burst frequency in WT (from 8.00 ± 1.13 bursts/min to 4.67 ± 0.53 bursts/min; p = 0.017) and no change in *Lmx1b*$^{f/f/p}$ preparations. We thus conclude that observations made in our experiments using 8-OH-DPAT were mediated by 5-HT$_{1a}$ receptor mechanisms and not confounded by action of this drug on 5-HT$_7$ receptors.

Coapplication of 8-OH-DPAT and glycinergic/GABAergic receptor antagonists

We hypothesized that a mechanism for the transient excitation caused by 8-OH-DPAT in *Lmx1b*$^{f/f/p}$ mice involves disinhibition of the respiratory network because downstream 5-HT$_{1a}$ receptors are predominantly located on inhibitory glycinergic respiratory interneurons including the preBötC inspiratory rhythm generator (Dutschmann et al., 2009; Manzke et al., 2009). Inhibition of these inhibitory neurons by 5-HT$_{1a}$ receptor-activation could cause network excitation. To test this hypothesis, experiments were performed with inhibitory receptor (glycinergic and GABAergic) antagonists in the *Lmx1b*$^{f/f/p}$ slice preparations to determine endogenous inhibitory control of the inspiratory bursting frequency, and to then test for occlusion of 8-OH-DPAT-induced excitation by the antagonists (Fig. 9). We first applied a mixture of gabazine (0.5 μM), CGP 55845 (1 μM) and strychnine (0.5 μM), respectively. In 8 of 11 preparations, these blockers significantly augmented inspiratory burst frequency (Fig. 9; average increase in frequency of 167%; one-way RM ANOVA, $p < 0.001$), indicating ongoing inhibitory control of the inspiratory rhythm. Subsequent coapplication of the inhibitory blocker mixture and 8-OH-DPAT (100 μM; n = 8 *Lmx1b*$^{f/f/p}$) did not cause a significant transient further increase in peak or steady-

state burst frequency, indicating that the inhibitory blockers effectively occluded the excitatory actions of 8-OH-DPAT.

Discussion

This study exploits a transgenic mouse model to differentiate and identify the roles in respiratory control of 5-HT$_{1a}$ autoreceptors located on serotonergic neurons, versus heteroreceptors located on downstream nuclei. The bulk of the evidence shows that 5-HT neurons have a net stimulatory effect on the respiratory network (for review, see Richerson, 2004; Hodges and Richerson, 2008a; Ptak et al., 2009; Depuy et al., 2011). However, it has alternately been proposed that the net effect of 5-HT is inhibitory (Lalley, 1986, 1994), or that 5-HT acts as a "modulator" of respiratory output (Hodges and Richerson, 2008a). We propose that the discrepancies regarding the effect of 5-HT on breathing resulted from expression of multiple 5-HT receptor subtypes at different locations with varying effects on respiratory output. In particular, activation of 5-HT$_{1a}$ receptors results in two competing effects: initial stimulation of breathing due to excitation of the respiratory network and a secondary decrease in stimulation of breathing due to silencing of 5-HT neurons.

Validation of the Lmx1b$^{f/f/p}$ mouse as a tool for studying 5-HT$_{1a}$ receptor distribution and functions

These experiments are the first time the *in vitro* rhythmic medullary slice preparation has been used from *Lmx1b*$^{f/f/p}$ mice (Zhao et al., 2006). Here we show that despite lacking >99% of central serotonergic neurons, slices prepared from neonatal *Lmx1b*$^{f/f/p}$ mice produced a relatively consistent, albeit altered, respiratory-related rhythmic discharge. There was a slower and more irregular hypoglossal inspiratory burst pattern than observed in WT preparations. This pattern of discharge is reminiscent of phrenic nerve recordings from the *in vitro* brainstem–spinal cord preparation of *Lmx1b*$^{f/f/p}$ mice (Hodges et al., 2009).

These findings were paralleled *in vivo*, where *Lmx1b*$^{f/f/p}$ neonates ventilate more slowly than WT siblings and with shallower breaths, and also exhibit an increased number of apneas (Hodges et al., 2009).

Interestingly, previous observations point to an absolute requirement for 5-HT in generation of the respiratory rhythm in neonatal mouse and rat slices (Peña and Ramirez, 2002; Ptak et al., 2009). In contrast, we recorded spontaneous respiratory bursting in slice preparations devoid of central 5-HT neurons, suggesting that there might be some compensatory mechanism in *Lmx1b*$^{f/f/p}$ mice to maintain respiratory output. However, our results indicate that this compensatory excitatory drive in *Lmx1b*$^{f/f/p}$ mice is not due to an increase in noradrenergic tone.

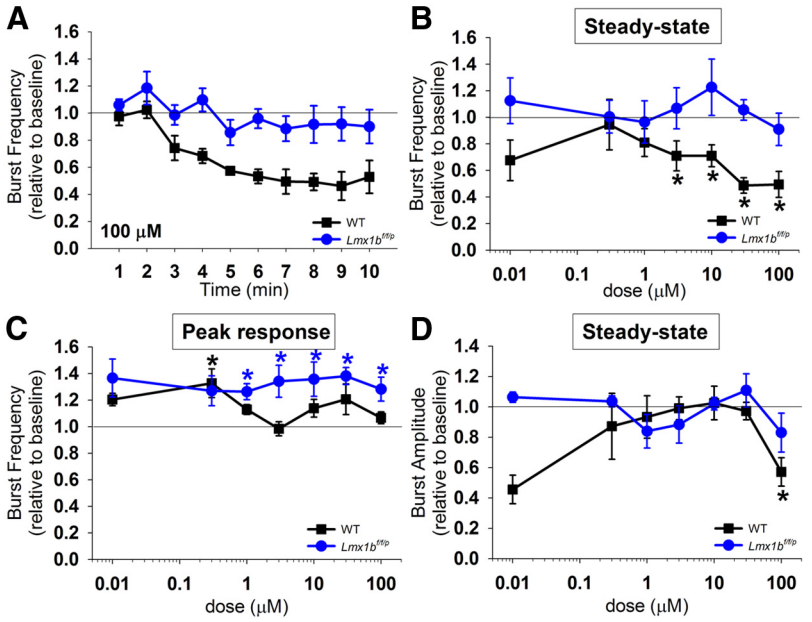

Figure 5. 8-OH-DPAT differentially affected hypoglossal nerve discharge in WT and *Lmx1b*$^{f/f/p}$ rhythmogenic slices. ***A***, Time course of burst frequency (relative to baseline) during a 10 min bath application of 8-OH-DPAT (100 μM) in WT and *Lmx1b*$^{f/f/p}$ slices. ***B***,***C***, 8-OH-DPAT dose–response curves (10 nM–100 μM) showing changes in burst frequency relative to baseline at steady-state (***B***) and during the peak response (***C***; $n = 3, 4, 4, 6, 6, 6, 5$ slices for each successive dose of 8-OH-DPAT in WT; $n = 4, 5, 4, 5, 4, 9, 5$ for each successive dose in *Lmx1b*$^{f/f/p}$). ***D***, Steady-state responses of burst amplitude (relative to baseline) at different doses of 8-OH-DPAT. *Significant difference from baseline; paired *t* test, $p < 0.05$). Data are mean ± SEM.

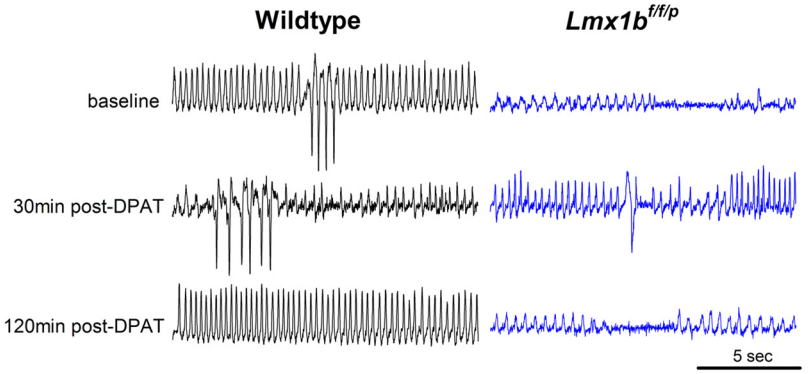

Figure 6. Ventilatory traces from whole-body plethysmographic recordings in WT and *Lmx1b*$^{f/f/p}$ P2 mouse pups at baseline, 30 min, and 120 min after subcutaneous injection of 100 μg/kg 8-OH-DPAT.

The maintenance of respiratory output could be due to an increase in other inputs, such as glutamatergic tonic drive (Crone et al., 2012), or there could be changes in expression of ion channels or synaptic connections within the respiratory network consistent with homeostatic plasticity reported in other systems (Turrigiano and Nelson, 2004; Marder and Goaillard, 2006).

In order for the *Lmx1b*$^{f/f/p}$ mouse to be a valid tool for differentiating between 5-HT$_{1a}$ autoreceptor and heteroreceptor function, it was necessary to confirm that the numbers of 5-HT neurons and their 5-HT$_{1a}$ autoreceptors were diminished. Evidence presented includes immunohistochemical staining for TpOH-positive cells, which revealed a >99% absence of 5-HT neurons in the medulla of *Lmx1b*$^{f/f/p}$ mice, in agreement with previous observations (Ding et al., 2003; Zhao et al., 2006). Additionally, there was a decrease in 5-HT$_{1a}$ receptor binding sites in raphe nuclei as assessed by autoradiography. Interestingly, the number of 5-HT$_{1a}$ receptors outside the raphe (which likely in-

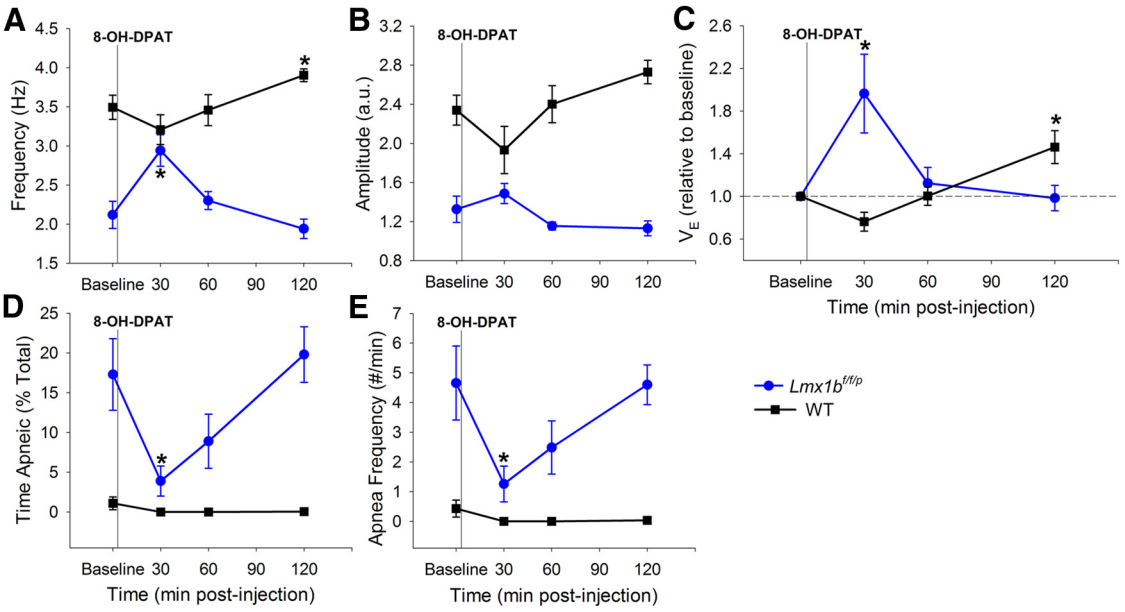

Figure 7. Breathing was augmented in neonatal mouse pups lacking central 5-HT neurons after injection of 8-OH-DPAT. ***A***, ***B***, Breathing frequency (***A***) and breath amplitude (***B***; index of tidal volume) before and after injection of 8-OH-DPAT in WT and *Lmx1b*$^{f/f/p}$ pups ($n = 7$ WT, $n = 7$ *Lmx1b*$^{f/f/p}$). ***C***, Minute ventilation (V_E) expressed relative to baseline. ***D***, ***E***, Percentage of time spent apneic (defined as a respiratory pause >1 s) (***D***) and frequency of apneas (***E***) before and after injection of 8-OH-DPAT. One-way RM ANOVA followed by Bonferroni *post hoc* for multiple comparisons, compared with baseline; $p < 0.05$. *Significant difference from baseline. Data are mean ± SEM.

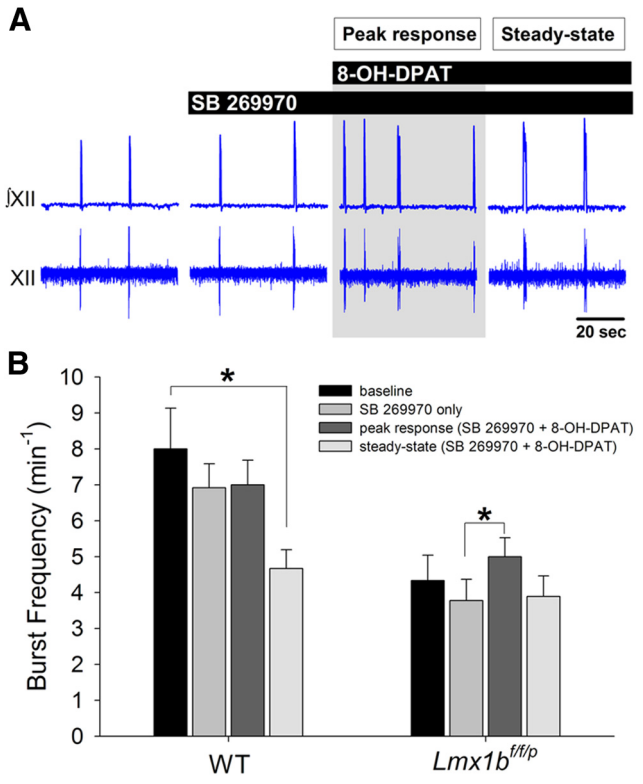

Figure 8. 8-OH-DPAT elicited a transient increase in frequency (peak response) in *Lmx1b*$^{f/f/p}$ preparations, despite concurrent blockade of 5-HT$_7$ receptors. ***A***, XII nerve and ∫XII nerve activity in an *Lmx1b*$^{f/f/p}$ slice during control conditions, bath application of SB 269970 (20 μM), and coapplication of SB 269970 and 8-OH-DPAT (3 μM). ***B***, Hypoglossal burst frequency at baseline, during application of SB 269970, and during coapplication of SB 269970 and 8-OH-DPAT ($n = 6$ WT, $n = 9$ *Lmx1b*$^{f/f/p}$). Shown are both the peak and steady-state responses to 8-OH-DPAT (attained at the end of 10 min of drug application; one-way RM ANOVA followed by Bonferroni *post hoc* for multiple comparisons; $p < 0.05$). *Significant difference. Data are mean ± SEM.

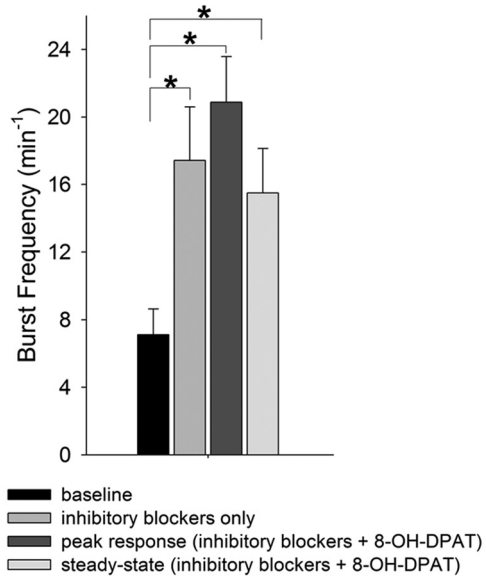

Figure 9. Inhibitory receptor blockers occluded the 8-OH-DPAT-induced excitation in *Lmx1b*$^{f/f/p}$ slice preparations. Hypoglossal burst frequency at baseline, during application of an inhibitory blocker mixture consisting of gabazine (0.5 μM), CGP 55845 (1 μM), and strychnine (0.5 μM), and during coapplication of inhibitory blockers and 8-OH-DPAT (100 μM; $n = 8$ *Lmx1b*$^{f/f/p}$). Shown are both the peak and steady-state responses to 8-OH-DPAT (attained at the end of 10 min of drug application; one-way RM ANOVA followed by Bonferroni *post hoc* for multiple comparisons; $p < 0.05$). *Significant difference. Data are mean ± SEM.

cluded the preBötC in the CVL sampled) remained unchanged, suggesting that the loss of 5-HT did not lead to upregulation or downregulation of 5-HT$_{1a}$ heteroreceptors in these areas. We also assessed the functional consequence of a loss of 5-HT neurons by demonstrating loss of the 5-HT$_{2a}$ receptor-mediated respiratory drive that normally stimulates the respiratory network (Peña and Ramirez, 2002; Ptak et al., 2009). The 5-HT$_{2a}$ receptor antagonist MDL 11939 (50 μM) reduced respiratory output in

slices from WT mice as expected, but had no effect in slices from *Lmx1b*$^{f/f/p}$ mice, consistent with the absence of endogenous 5-HT.

These data support the use of this mouse as a unique tool to investigate the effect of activating downstream 5-HT$_{1a}$ heteroreceptors on respiratory output in the absence of a confounding effect of 5-HT neuron inhibition by activation of 5-HT$_{1a}$ autoreceptors.

Differentiation of inhibitory autoreceptor and downstream heteroreceptor activation in respiratory control

5-HT$_{1a}$ receptors are widely distributed throughout the brain including regions involved in respiration such as the preBötC, retrotrapezoid nucleus/ parafacial respiratory group, raphe nuclei, nucleus of the solitary tract, and hypoglossal nuclei (Liu and Wong-Riley, 2010). Those receptors located on raphe serotonergic cells serve a unique function, providing autoinhibition via negative feedback (McCall and Clement, 1989; Sharp et al., 1989; Veasey et al., 1995; Aghajanian and Sanders-Bush, 2002).

Our results demonstrate downstream excitation of respiratory output via 5-HT$_{1a}$ heteroreceptors. Using *Lmx1b*$^{f/f/p}$ mice, in which only downstream 5-HT$_{1a}$ heteroreceptors exist, we found that 8-OH-DPAT increased ventilation *in vivo*, and increased hypoglossal inspiratory burst frequency *in vitro*. These observations are consistent with previous work demonstrating that 5-HT$_{1a}$ receptors facilitate breathing via involvement in the hypoxic ventilatory response (Hilaire and Duron, 1999; Bou-Flores et al., 2000; Nucci et al., 2008) and in the counteraction of respiratory depression caused by spontaneous central apneas, apneusis, and opioid-induced ventilatory depression (Lalley et al., 1994; Sahibzada et al., 2000; Meyer et al., 2006; Stettner et al., 2008; Dutschmann et al., 2009; Guenther et al., 2009; Manzke et al., 2009). The latter compensation was confirmed as 5-HT$_{1a}$ receptor activation since the effect of 8-OH-DPAT was blocked by WAY-100635 (a 5-HT$_{1a}$ receptor antagonist). Other 5-HT$_{1a}$ agonists have also been used to treat apneusis and apneic periods (Wilken et al., 1997; El-Khatib et al., 2003).

The mechanisms for downstream excitation of the respiratory system are unclear. 5-HT$_{1a}$ receptors are coupled to inhibitory G-proteins (Raymond et al., 1999), so a potential mechanism for the excitatory action of 8-OH-DPAT is through disinhibition of the respiratory network. Downstream 5-HT$_{1a}$ receptors are predominantly located on inhibitory glycinergic respiratory interneurons, therefore their activation by a ligand would inhibit those inhibitory neurons, resulting in excitation (Dutschmann et al., 2009; Manzke et al., 2009). This could possibly also involve a complex reorganization of respiratory network operation *in vivo* (Shevtsova et al., 2011). This hypothesis of network disinhibition was confirmed by the occlusion of 8-OH-DPAT-induced excitation by inhibitory receptor (glycinergic and GABAergic) antagonists (Fig. 9).

In contrast, 8-OH-DPAT depressed breathing activity in WT mice *in vivo*, and in WT slices *in vitro*. WT mice have 5-HT$_{1a}$ autoreceptors and heteroreceptors, thus interpretation of 8-OH-DPAT data must consider the net effect of both types of 5-HT$_{1a}$ receptors. Pharmacological activation of 5-HT$_{1a}$ receptors in the medullary raphe decreases 5-HT neuron firing and reduces heart rate and ventilation (Ootsuka and Blessing, 2006; Nakamura and Morrison, 2007). Additionally, activation of inhibitory 5-HT$_{1a}$ autoreceptors by focal injection of 8-OH-DPAT into the raphe results in blunting of the hypercapnic ventilatory response (Messier et al., 2004; Taylor et al., 2005). The action of 5-HT$_{1a}$ autoreceptors is further demonstrated by their involvement in other autonomic functions. Mice with excessive 5-HT inhibition due to overexpression of 5-HT$_{1a}$ in serotonin reuptake transporter-expressing cells exhibit sporadic autonomic crises and increased spontaneous death occurring between P25 and P80 (Audero et al., 2008). Our results demonstrate that in neonatal mice, the inhibitory 5-HT$_{1a}$ autoreceptor effect of 8-OH-DPAT dominates over the downstream excitatory effect. The inhibition of 5-HT neurons via autoreceptor activation and resulting decrease in endogenous serotonin release onto downstream excitatory 5-HT$_{2a}$ receptors can explain the observed depression in respiratory motor output.

Distinguishing between downstream mechanisms

We have ruled out the possibility that the moderate affinity of 5-HT$_7$ receptors for 8-OH-DPAT (Bard et al., 1993; Eriksson et al., 2008) could explain the excitatory action on respiration. Not much is known regarding the role of 5-HT$_7$ in breathing, however, this G-protein coupled receptor is positively linked to adenylate cyclase, is expressed in the preBötC, and has been detected in the raphe magnus. It colocalizes with 5-HT neurons and is involved in restoring phrenic nerve activity following fentanyl-induced depression of respiratory discharge (Barnes and Sharp, 1999; Muneoka and Takigawa, 2003; Richter et al., 2003). We administered a 5-HT$_7$ antagonist (SB 269970) alone, and then with 8-OH-DPAT to isolate the effect of the latter drug on 5-HT$_{1a}$ receptors. A similar approach has been used previously in studies on thermoregulation and learning (Hedlund et al., 2004; Faure et al., 2006; Eriksson et al., 2008). SB 269970 alone did not alter hypoglossal output in either *Lmx1b*$^{f/f/p}$ or WT preparations. It also failed to inhibit the 8-OH-DPAT-induced increase in frequency observed in *Lmx1b*$^{f/f/p}$ preparations, supporting the conclusion that downstream 5-HT$_{1a}$ receptors facilitate breathing.

Our study provides a unique view identifying which receptors mediate the effect of 8-OH-DPAT on respiration, and rule out 5-HT$_7$ receptors as targets of 8-OH-DPAT in the context of respiratory control. Our results argue the need for cautious interpretation when using 8-OH-DPAT as a 5-HT$_{1a}$ agonist in respiratory control studies. We confirm differential roles for 5-HT$_{1a}$ receptors in breathing, depending on their synaptic location. There is a dominant inhibitory effect due to inhibition of 5-HT neurons, and a stimulatory effect on the respiratory network due to activation of 5-HT$_{1a}$ heteroreceptors. The latter stimulatory effect would be the dominant effect when 5-HT is released under normal conditions *in vivo*.

References

Aghajanian GK, Sanders-Bush E (2002) Serotonin. In: Neuropsychopharmacology: the fifth generation of progress (Davis KL, Charney D, Coyle JT, Nemeroff C, eds), pp 15–34. Philadelphia: Lippincott Williams and Wilkins.

Audero E, Coppi E, Mlinar B, Rossetti T, Caprioli A, Banchaabouchi MA, Corradetti R, Gross C (2008) Sporadic autonomic dysregulation and death associated with excessive serotonin autoinhibition. Science 321:130–133. CrossRef Medline

Bard JA, Zgombick J, Adham N, Vaysse P, Branchek TA, Weinshank RL (1993) Cloning of a novel human serotonin receptor (5-HT7) positively linked to adenylate cyclase. J Biol Chem 268:23422–23426. Medline

Barnes NM, Sharp T (1999) A review of central 5-HT receptors and their function. Neuropharmacology 38:1083–1152. CrossRef Medline

Bou-Flores C, Lajard AM, Monteau R, De Maeyer E, Seif I, Lanoir J, Hilaire G (2000) Abnormal phrenic motoneuron activity and morphology in neonatal monoamine oxidase A-deficient transgenic mice: possible role of a serotonin excess. J Neurosci 20:4646–4656. Medline

Buchanan GF, Richerson GB (2010) Central serotonin neurons are required for arousal to CO_2. Proc Natl Acad Sci U S A 107:16354–16359. CrossRef Medline

Crone SA, Viemari JC, Droho S, Mrejeru A, Ramirez JM, Sharma K (2012) Irregular breathing in mice following ablation of V2a neurons. J Neurosci 32:7895–7906. CrossRef Medline

Cummings KJ, Pendlebury JD, Sherwood NM, Wilson RJ (2004) Sudden neonatal death in PACAP-deficient mice is associated with reduced respiratory chemoresponse and susceptibility to apnoea. J Physiol 555:15–26. CrossRef Medline

Depuy SD, Kanbar R, Coates MB, Stornetta RL, Guyenet PG (2011) Control of breathing by raphe obscurus serotonergic neurons in mice. J Neurosci 31:1981–1990. CrossRef Medline

Ding YQ, Marklund U, Yuan W, Yin J, Wegman L, Ericson J, Deneris E, Johnson RL, Chen ZF (2003) Lmx1b is essential for the development of serotonergic neurons. Nat Neurosci 6:933–938. CrossRef Medline

Dutschmann M, Waki H, Manzke T, Simms AE, Pickering AE, Richter DW, Paton JFR (2009) The potency of different serotonergic agonists in counteracting opioid evoked cardiorespiratory disturbances. Philos Trans Lond B Biol Sci 364:2611–2623. CrossRef Medline

El-Khatib MF, Kiwan RA, Jamaleddine GW (2003) Buspirone treatment for apneustic breathing in brain stem infarct. Respir Care 48:956–958. Medline

Eriksson TM, Golkar A, Ekström JC, Svenningsson P, Ogren SO (2008) 5-HT$_7$ receptor stimulation by 8-OH-DPAT counteracts the impairing effect of 5-HT$_{1A}$ receptor stimulation on contextual learning in mice. Eur J Pharmacol 596:107–110. CrossRef Medline

Faure C, Mnie-Filali O, Scarna H, Debonnel G, Haddjeri N (2006) Effects of the 5-HT7 receptor antagonist SB-269970 on rat hormonal and temperature responses to the 5-HT1A/7 receptor agonist 8-OH-DPAT. Neurosci Lett 404:122–126. CrossRef Medline

Guenther U, Manzke T, Wrigge H, Dutschmann M, Zinserling J, Putensen C, Hoeft A (2009) The counteraction of opioid-induced ventilatory depression by the serotonin 1A-agonist 8-OH-DPAT does not antagonize antinociception in rats in situ and in vivo. Anesth Analg 108:1169–1176. CrossRef Medline

Hedlund PB, Kelly L, Mazur C, Lovenberg T, Sutcliffe JG, Bonaventure P (2004) 8-OH-DPAT acts on both 5-HT1a and 5-HT7 receptors to induce hypothermia in rodents. Eur J Pharmacol 487:125–132. CrossRef Medline

Hilaire G, Duron B (1999) Maturation of the mammalian respiratory system. Physiol Rev 79:325–360. Medline

Hodges MR, Richerson GB (2008a) Contributions of 5-HT neurons to respiratory control: neuromodulatory and trophic effects. Respir Physiol Neurobiol 164:222–232. CrossRef Medline

Hodges MR, Richerson GB (2008b) Interaction between defects in ventilatory and thermoregulatory control in mice lacking 5-HT neurons. Respir Physiol Neurobiol 164:350–357. CrossRef Medline

Hodges MR, Tattersall GJ, Harris MB, McEvoy SD, Richerson DN, Deneris ES, Johnson RL, Chen ZF, Richerson GB (2008) Defects in breathing and thermoregulation in mice with near-complete absence of central serotonin neurons. J Neurosci 28:2495–2505. CrossRef Medline

Hodges MR, Wehner M, Aungst J, Smith JC, Richerson GB (2009) Transgenic mice lacking serotonin neurons have severe apnea and high mortality during development. J Neurosci 29:10341–10349. CrossRef Medline

Hodges MR, Best S, Richerson GB (2011) Altered ventilatory and thermoregulatory control in male and female adult *Pet-1* null mice. RespIR Physiol Neurobiol 177:133–140. CrossRef Medline

Lalley PM (1986) Serotonergic and non-serotonergic responses of phrenic motoneurones to raphé stimulation in the cat. J Physiol 380:373–385. Medline

Lalley PM (1994) The excitability and rhythm of medullary respiratory neurons in the cat are altered by the serotonin receptor agonist 5-methoxy-*N*-*N*, dimethyltryptamin. Brain Res 648:87–98. CrossRef Medline

Lalley PM, Bischoff AM, Richter DW (1994) 5-HT-1A receptor-mediated modulation of medullary expiratory neurones in the cat. J Physiol 476: 117–130. Medline

Liu Q, Wong-Riley MT (2010) Postnatal changes in the expressions of serotonin 1A, 1B and 2A receptors in ten brain stem nuclei of the rat: implication for a sensitive period. Neuroscience 165:61–78. CrossRef Medline

Manzke T, Dutschmann M, Schlaf G, Mörschel M, Koch UR, Ponimaskin E, Bidon O, Lalley PM, Richter DW (2009) Serotonin targets inhibitory synapses to induce modulation of network functions. Philos Trans R Soc Lond B Biol Sci 364:2589–2602. CrossRef Medline

Marder E, Goaillard JM (2006) Variability, compensation and homeostasis in neuron and network function. Nat Rev Neurosci 7:563–574. CrossRef Medline

McCall RB, Clement ME (1989) Identification of serotonergic and sympathetic neurons in medullary raphé nuclei. Brain Res 477:172–182. CrossRef Medline

Messier ML, Li A, Nattie EE (2004) Inhibition of medullary raphé serotonergic neurons has age-dependent effects on the CO_2 in newborn piglets. J Appl Physiol 96:1909–1919. CrossRef Medline

Meyer LC, Fuller A, Mitchell D (2006) Zacopride and 8-OH-DPAT reverse opioid-induced respiratory depression and hypoxia but not catatonic immobilization in goats. Am J Physiol Regul Integr Comp Physiol 290: R405–R413. CrossRef Medline

Muneoka KT, Takigawa M (2003) 5-Hydroxytryptamine7 (5-HT7) receptor immunoreactivity-positive "stigmoid body"-like structure in developing rat brains. Int J Dev Neurosci 21:133–143. CrossRef Medline

Nakamura K, Morrison SF (2007) Central efferent pathways mediating skin cooling-evoked sympathetic thermogenesis in brown adipose tissue. Am J Physiol Regul Integr Comp Physiol 292:R127–R136. CrossRef Medline

Nucci TB, Branco LG, Gargaglioni LH (2008) 5-HT1A, but not 5-HT2 and 5-HT7, receptors in the nucleus raphé magnus modulate hypoxia-induced hyperpnoea. Acta Physiol (Oxf) 193:403–414. CrossRef Medline

Okabe S, Mackiewicz M, Kubin L (1997) Serotonin receptor mRNA expression in the hypoglossal motor nucleus. Respir Physiol 110:151–160. CrossRef Medline

Ootsuka Y, Blessing WW (2006) Thermogenesis in brown adipose tissue: increase by 5-HT2A receptor activation and decrease by 5-HT1A receptor activation in conscious rats. Neurosci Lett 395:170–174. CrossRef Medline

Peña F, Ramirez JM (2002) Endogenous activation of serotonin-2A receptors is required for respiratory rhythm generation in vitro. J Neurosci 22:11055–11064. Medline

Ptak K, Yamanishi T, Aungst J, Milescu LS, Zhang R, Richerson GB, Smith JC (2009) Raphé neurons stimulate respiratory circuit activity by multiple mechanisms via endogenously released serotonin and substance P. J Neurosci 29:3720–3737. CrossRef Medline

Raymond JR, Mukhin YV, Gettys TW, Garnovskaya MN (1999) The recombinant 5-HT1A receptor: G protein coupling and signaling pathways. Br J Pharmacol 127:1751–1764. CrossRef Medline

Richerson GB (2004) Serotonergic neurons as carbon dioxide sensors that maintain pH homeostasis. Nat Rev Neurosci 5:449–461. CrossRef Medline

Richter DW, Manzke T, Wilken B, Ponimaskin E (2003) Serotonin receptors: guardians of stable breathing. Trends Mol Med 9:542–548. CrossRef Medline

Sahibzada N, Ferreira M, Wasserman AM, Taveira-DaSilva AM, Gillis RA (2000) Reversal of morphine-induced apnea in the anesthetized rat by drugs that activate 5-hydroxytryptamine(1A) receptors. J Pharmacol Exp Ther 292:704–713. Medline

Sharp T, Bramwell SR, Grahame-Smith DG (1989) 5-HT$_1$ agonists reduce 5-hydroxytryptamine release in rat hippocampus in vivo as determined by brain microdialysis. Br J Pharmacol 96:283–290. CrossRef Medline

Shevtsova NA, Manzke T, Molkov YI, Bischoff A, Smith JC, Rybak IA, Richter DW (2011) Computational modelling of 5-HT receptor-mediated reorganization of the brainstem respiratory network. Eur J Neurosci 34:1276–1291. CrossRef Medline

Smith JC, Ellenberger HH, Ballanyi K, Richter DW, Feldman JL (1991) Pre-Bötzinger complex: a brainstem region that may generate respiratory rhythm in mammals. Science 254:726–729. CrossRef Medline

Stettner GM, Zanella S, Hilaire G, Dutschmann M (2008) 8-OH-DPAT suppresses spontaneous central apneas in the C57BL/6J mouse strain. Respir Physiol Neurobiol 161:10–15. CrossRef Medline

Taylor NC, Li A, Nattie EE (2005) Medullary serotonergic neurones modulate the ventilatory response to hypercapnia, but not hypoxia in conscious rats. J Physiol 566:543–557. CrossRef Medline

Turrigiano GG, Nelson SB (2004) Homeostatic plasticity in the developing nervous system. Nat Rev Neurosci 5:97–107. CrossRef Medline

Veasey SC, Fornal CA, Metzler CW, Jacobs BL (1995) Response of serotonergic caudal raphé neurons in relation to specific motor activities in freely moving cats. J Neurosci 15:5346–5359. Medline

Viemari JC, Garcia AJ 3rd, Doi A, Ramirez JM (2011) Activation of alpha-2 noradrenergic receptors is critical for the generation of fictive eupnea and fictive gasping inspiratory activities in mammals *in vitro.* Eur J Neurosci 33:2228–2237. CrossRef Medline

Wilken B, Lalley P, Bischoff AM, Christen HJ, Behnke J, Hanefeld F, Richter DW (1997) Treatment of apneustic respiratory disturbance with a serotonin-receptor agonist. J Pediatr 130:89–94. CrossRef Medline

Zhao ZQ, Scott M, Chiechio S, Wang JS, Renner KJ, Gereau RW 4th, Johnson RL, Deneris ES, Chen ZF (2006) Lmx1b is required for maintenance of central serotonergic neurons and mice lacking central serotonergic system exhibit normal locomotor activity. J Neurosci 26:12781–12788. CrossRef Medline